Quantification of tablet sensitivity to a stress concentration: Generalization of Hiestand's approach and link with the microstructure

B. Croquelois, J. Girardot, J.B. Kopp, P. Tchoreloff, V. Mazel

1   **Quantification of tablet sensitivity to a stress concentration: generalization of**

2   **Hiestand's approach and link with the microstructure**

3   B. Croquelois[1], J. Girardot[2], J.B. Kopp[2], P. Tchoreloff[1], V. Mazel[1,*]

4

5   [1] Univ. Bordeaux, CNRS, Arts et Metiers Institute of Technology, Bordeaux INP, INRAE,

6   I2M Bordeaux, F-33400 Talence, France

7   [2] Arts et Metiers Institute of Technology, University of Bordeaux, CNRS, Bordeaux INP,

8   INRAE, I2M Bordeaux, F-33400 Talence, France.

9   * Corresponding author: address: I2M, Univ. Bordeaux, 146 rue Léo Saignat,   F-33000

10 Bordeaux, France ; tel :+33 5 57 57 15 39 ; E-mail address: vincent.mazel@u-bordeaux.fr

11 **Abstract**

12 Sensitivity to a stress concentration is important for the development of pharmaceutical

13 tablets as it is related to defects like capping. The Brittle Fracture Index (BFI) was

14 introduced by Hiestand *et al.* to test this sensitivity. Recently, a more general index,

15 based on the average stress criterion, was proposed as a generalized Hiestand

16 approach. In this work, this new approach is tested on tablets obtained for several

17 products and pressure levels, and results show the wide applicability of the new

18 criterion.

19 Furthermore, X-ray micro-computed tomography was used to link the tablet

20 microstructure and the sensitivity to a stress concentration. A strong correlation was

21 found between the size of the largest pores in the structure and the value of a_0 which

22 quantify the sensitivity to a stress concentration in the generalized Hiestand approach.

These results constitute the first attempt to link the brittle fracture propensity of tablets with their effective microstructure.

1. Introduction

Tableting is a common process for the production of pharmaceutical dosage forms. Manufacturing of tablets using die compaction have been used for more than a century. Nevertheless, despite an apparent simplicity, the process of compaction involves complicated mechanical phenomena, both reversible and non-reversible. The properties of the final tablets are the consequence of complex interactions between the powder properties (material parameters) and the process parameters. The characterization of the behavior of a formulation during compaction is generally performed by studying the evolution of the tablet porosity and mechanical strength (measured generally by diametral compression) as a function of the pressure used to make the tablet [1]. These characterizations are now summarized in the US Pharmacopeia under the terms compressibility, tabletability and compactibility [2].

One of the main challenge for the manufacturing of pharmaceutical tablet is to avoid the occurrence of classical problems like capping or lamination during scale-up [3]. Unfortunately, the previously described characterizations are not always sufficient to predict the occurrence of these kinds of defects. The case of capping, which, in the case of biconvex tablet, corresponds to the breakage of at least one of the tablet cups, is particularly difficult to predict. From a mechanistic point of view, it is due to the development, during the unloading phase, of a high shear stress at the limit between the

46 land and the cup of the tablet (Hiestand et al., 1977; Mazel et al., 2015; Wu et al., 2008).

47 This stress is highly concentrated and it is well known that the prediction of the breakage

48 of a solid under concentrated stress is more difficult than in the case of homogeneous

49 stresses [7].

50 To overcome this problem, Hiestand et al. proposed the introduction of another

51 parameter for the characterization of a formulation: the brittle fracture index (BFI) [4].

52 This index is calculated by comparing the tensile stress of a tablet with the apparent

53 tensile strength of a tablet obtained under the same conditions but containing a hole at

54 its center. The presence of the hole promotes the development of stress concentrations

55 near the hole edge. By comparing the two values it becomes possible to study the

56 sensitivity of a formulation concentrated stresses. Several examples of studies using this

57 approach can be found in the literature [8–13]. It can be noted that the sensitivity to a

58 stress concentration is sometimes called brittleness [14]. Nevertheless, other articles in

59 the pharmaceutical literature refers also to brittleness with a slightly different meaning.

60 For example, in some cases, a more brittle tablet is said to be more friable [15–18]. In

61 other studies the brittleness of a tablet is directly linked with the stress intensity factor

62 (resistance of a material to the propagation of a crack)[19]. The sensitivity to a stress

63 concentration do not correspond to neither of these concepts. For this reason, the term

64 brittleness will be avoided in the present paper.

65 If BFI is of interest, it is unfortunately dependent of the size of the hole introduced in the

66 tablet. As a consequence, results published in the literature are difficult to compare one

67 to another. For this reason, we recently proposed to introduce a new index, calculated

68 using different hole sizes, in order to generalize Hiestand's approach [20]. Using the

average stress criterion introduced by Whitney et al.[7], it was found possible to characterize the evolution of the strength of the tablet as a function of the hole size. A new parameter, a_0, which is a characteristic distance, could be used to replace the BFI and quantify the sensitivity of a product to a stress concentration. In our previous work, only two products compacted at one compaction pressure were studied to see the applicability of the criterion. In the present work, the criterion is applied to tablets obtained for five different products under at least three different compaction pressures to verify the applicability of the criteria using a broader set of samples. Changing the compaction pressure would also make it possible to study the evolution of the sensitivity to a stress concentration as a function of the porosity of the tablet.

Then, the second objective of this study is to go further than only a descriptive index and to try to understand the relationship between the sensitivity to a stress concentration and the microstructure of the tablet. For this purpose, X-ray microcomputed-tomography (XμCT) was used to study the tablet microstructure as commonly done in the literature [21–24]. A special focus was made on the size of the biggest pores in the structure that are susceptible to play an important role in the failure mechanism [25,26].

2. Material and methods

2.1. Powders

Five different powders were used to produce compacts: calcium phosphate dihydrate (DCP) (Dicafos D160, Chemische Fabrik Budenheim Budenheim, Germany), granulated α-lactose monohydrate (MLac) (Excipress, Armor Pharma, France), anhydrous β-latose (ALac) (Duralac, Meggle, Wasserburg, Germany), spray-dried lactose monohydrate (SDLac) (SuperTab 14SD, FSD) and spray-dried mannitol (SDMan) (Pearlitol, Roquette,

Lastreme, France). Table 1 and figure 1 present the particle size distribution data and photographs obtained using scanning electron microscope for the different products. It is worth noting that tablets of these products present brittle failure when broken in diametral compression. To perform the compaction experiments, the products were mixed with 1% (w/w) of magnesium stearate (Cooper, Melun, France) to minimize the frictions in the die. The blending was performed at 49 rpm for 5 min using a turbula mixer (Type T2C, Willy A Bachofen, Muttenz, Switzerland).

2.2. Tablet compaction

All the compacts were produced using a compaction simulator Stylcam® (Medelpharm, Beynost, France). This tableting press is a single station press. It is equipped with force sensors (accuracy 10 N) and the displacements of the punches are monitored with an accuracy of 0.01 mm.

For the application of the generalized Hiestand's approach, a special set of flat faced Euro B tooling was used as described previously [20,27]. These tooling made it possible to obtained a so-called flattened geometry. In the present study, tablets with a diameter of 11mm were used with a flat end of 30°[27]. All the compacts were obtained using the same compaction kinematic (total compression time of about 100 ms). Compression pressures of 100, 200, 300 and 400 MPa were used to produce the tablets. For SDLac and SDMan, tablets obtained under 400 MPa were too strong to be broken on the device described thereafter and were, as a consequence, not used. To avoid any effect due to the thickness, all the compacts manufactured had similar thicknesses around 3.0 mm. The density was calculated using the weight and dimensions of the compacts.

For XμCT, tablets with a diameter of 8 mm and a thickness of 2mm were produced under the same compaction conditions. Tablets were then cut using a sharp blade knife to obtain small cubes of about 2x2x2 mm^3. The small cubes were taken from the center of the tablet as shown is figure 2.

2.3. Tablet machining

As described elsewhere [20], the holes in the tablets were inserted using a drill Micromot 50 E/EF (PROXXON S.A., Luxembourg). Three drill diameters (0.5, 0.8 and 1 mm) were used to make the holes. Machining speed was adapted for each product and each compaction pressure. The tablets were maintained using a specially designed polymeric holder obtained by 3D printing. Furthermore, a Polytetrafluoroethylene sheet was used to limit friction between the tablet and the piece holder. To avoid defects at the back of the tablet during machining holes, two tablets were placed together and only the upper one was finally used for experiments.

2.4. Tablet mechanical characterization

The diametral compression test was performed using a TA.HDplus texture analyzer (Stable microsystems, Surrey, United Kingdom). Compacts were compressed between two flat surfaces at a constant speed of 0.1 mm.s^{-1} with an acquisition frequency of 500 Hz. For each condition, ten compacts were broken.

2.5. X-ray tomography

Tablets were scanned using a lab-based system at PLACAMAT (UMS 3626, Pessac, France). The facility used was a GE VTomex-s with a xs-180-nf transmission source and

a diamond target. The scan parameters (voltage and intensity) were adapted for each sample. The 1800 projections for a 360° rotation were recorded using a binning factor of 1 and an exposure time of 1 second (total scanning time of two hours). The final voxel size was about 2.5µm for all the samples. Tomographic reconstructions were performed using phoenix-datos-x2 software with default parameters. Following image treatments were performed using the software Avizo V9 (Thermo Fisher Scientific, Waltham, USA). A cube of about 1.5x1.5x1.5 mm^3 was extracted from the data and submitted to further analyses. Details about the analyses will be given in the result part of the article.

3. Results and discussion

3.1. Application of the average stress criterion as a generalized Hiestand's approach

The five products were tested according to the methodology defined in our previous work [20]. For each product and each pressure point, tablets without hole and with holes of 0.5, 0.8 and 1 mm were broken and the breakage force was recorded. As all the tablets had the same size, analysis could be performed without transforming the forces into stresses. The ratio of the force needed to break the tablet with a hole to the force needed to break the tablet without a hole was then plotted as a function of the hole radius. Results can be found in figure 3. As expected, the ratio calculated is always below 1, which means that introducing a defect in the structure render the structure weaker. Moreover, the ratio is decreasing with increasing hole size in nearly all the cases (except for MLac between 300 MPa and 400 MPa for which the trend was not so clear). These results confirms the results published previously [20]. It also confirms that

158   the BFI defined by Hiestand *et al.*, which is calculated using the ratio, is dependent on

159   the hole size. This is true for all the products and for all the pressure points.

160   The other result is that, for each hole size, the ratio is decreasing with increasing

161   compaction pressure, i.e. with decreasing tablet porosity in nearly all the cases (except

162   for DCP at 100 and 200 MPa). This means that when the porosity decreases, the tablets

163   becomes more sensitive to a stress concentration. Similar results can be found in the

164   literature [4,11]. These results emphasize the relation between tablet microstructure and

165   sensitivity to a stress concentration. This aspect will be discussed in the last part of the

166   article.

167   The average stress criterion previously discussed was then used to represent the

168   evolution of the breakage force ratio as a function of the hole size. Results of the curve

169   fitting with the equation of the average stress criterion[20] can be seen in figure 3. As the

170   curve used to fit the data is non-linear, it is tedious to judge the quality of the fit using R^2

171   [28]. As an alternative, the value of the residual standard deviation (Se) is reported in

172   table 2 and was calculated as follow[29,30]:

173
$$Se = \sqrt{\frac{\sum_{i=1}^{N}(y_i - \hat{y_i})^2}{N - 1}}$$

174   With N the number of points used for the regression (3 in our case, for the 3 holes

175   sizes), y_i the ith experimental value and $\hat{y_i}$ the ith value predicted by the model. As it can

176   be seen in most of the cases, the curve fits correctly the experimental data. For

177   example, the agreement is very good for ALac and SDMan, and MLac gives the poorest

178   agreement especially for the highest pressure.

179 As the criterion makes it possible to correctly represent the evolution of the force ratio as

180 a function of the hole size, the a_0 parameters was extracted for each tablet set. Results

181 can be found in table 2. In accordance with the previous discussion, a_0 values

182 decreased (i.e. the sensitivity to a stress concentration increased) with increasing

183 compaction pressure (except for DCP at 100 and 200 MPa as previously). This

184 parameter can also be used to compare the products one to the other. For example, if

185 we compare the tablets obtained under 200MPa for each product, DCP has the highest

186 a_0, i.e. is the less sensitive to a stress concentration, whereas the lowest value of a_0 is

187 obtained for SDMan. In a similar way we can see that MLac and ALac have a similar

188 behavior regarding the stress concentration (except at the lowest pressure where ALac

189 is a more sensitive).

190 The results presented previously show that the average stress criterion can be used as

191 a generalized Hiestand's approach to characterize the sensitivity of a tablet to a stress

192 concentration. It would now be interesting to understand this sensitivity. From a

193 fundamental point of view, the sensitivity to a stress concentration should be related to

194 the tablet microstructure. The pores that are present in the microstructure play the role

195 of defects and are responsible of stress concentrations. If a structure has a lot of pores,

196 it means that it has a lot of defects. We can thus anticipate that it will be less sensitive to

197 the introduction of a hole in terms of strength (because it is already weakened by the

198 presence of the pores). This explains why, when the pressure increases, a_0 decreases.

199 When the pressure increases, the porosity of the tablets decreases (table 2) which

200 means that the concentration of defects in the structure decreases. As a consequence,

201 the tablet becomes more sensitive to a defect introduction and a_0 decreases, as it can
202 be observed in table 2.

203 This interpretation gives a first link between the tablet microstructure and its propensity
204 to brittle fracture. Nevertheless, global porosity is only a macroscopic description of the
205 microstructure in terms of global defect concentration. It does not give any information of
206 the actual geometry of the pores for example. When comparing the same product at
207 different porosity level, it can be supposed that the pores in the structure would be
208 comparable in terms of geometry. Nevertheless, when comparing two different products,
209 even if they have the same porosity level, it does not mean that the pore structure is the
210 same in terms of pore size for example. To illustrate this fact, table 3 present an
211 extraction of table 2 with all the tablets having a porosity level around 12.5% (11.3 to
212 13.8%). As it can be seen, very different a_0 values are obtained for the different
213 products, and no correlation can be found with the porosity variation. Porosity is thus not
214 a sufficient parameter to explain the sensitivity to a stress concentration of a tablet.

215

216 To understand the difference between the products at least two factors can be
217 considered. First it could be related with microscopic interaction between the grains.
218 This interaction being different from one product to another, it could explain the different
219 sensitivity to a stress concentration. The second factor could be related with the pore
220 structure itself. For example, the pore size varies from one product to another, even if
221 the global porosity is the same. Pores of different sizes represent very different kinds of
222 defects in the structure and might have different influence in terms of sensitivity to a

223 stress concentration[25]. To further explore the influence of pore structure on the

224 mechanical behavior of the tablet, XµCT was used in the following part.

3.2. Analysis of the pore structure using XµCT and link with the sensitivity to stress concentration

227 The purpose of this part was to further explore the influence of the pore structure on the

228 sensitivity to stress concentration. For the characterization of the pore structure we

229 focused our attention on the size of the pores, and more exactly on the size of the

230 biggest pores in the structure. The reason for that is the following. In terms of defects, it

231 is well-known the large defects have more influence on the actual strength of a structure

232 than small defects [25,26]. This was, for example, seen on the results shown above,

233 where larger hole diameters promote a larger decrease of the force needed to break the

234 tablet. It can thus be supposed that if a tablet contains large pores, it is already

235 weakened by these pores and as a consequence, it should be less sensitive to the

236 introduction of the central hole. We can thus suppose that a tablet with larger pores will

237 have a larger value of a_0 than a tablet that has smaller pores (supposing that the global

238 porosity is constant). The aim of this part was to test this hypothesis.

3.2.1. XµCT analysis protocol of the tablet

240 A procedure was thus defined in order to have an estimation of the dimensions of the

241 largest pores in the structure. The first step was to isolate the porosity in the XµCT

242 images. This required the use of a threshold in terms of grayscale that will separate the

243 solid from the pores. In the present study, the threshold was chosen in order to have, in

244 the numerical analysis of the XµCT images, a total porosity equal to the global porosity

measured on the analyzed tablets as presented in table 2. A typical example of the pore localization using this procedure can be found in figure 4. It is important to note that, in our case, only the biggest pores will be taken into consideration. These pores are those which are the less influenced by the thresholding procedure.

Afterwards, automatic procedures of the Avizo software were used to analyze the obtained pores in terms of size. First a complete 3D analysis was intended. Nevertheless, analysis showed a large connectivity of the pore structure (i.e. more of 60% of the pores was considered to be one single pore) and this did not make it possible to isolate easily the different pores in the structure. So instead of a real 3D analysis, a 2D+1 analysis was performed (i.e. a 2D analysis of images positioned along the third direction). For each slice of the XµcT results (each analysis contained approximately 600 slices), a 2D analysis of the pores was performed. For each pore an equivalent diameter was calculated which corresponds to the diameter of the disc that would have the same surface as the pore. This diameter was taken as the characteristic size of the pores. Other parameters like the form factor were also calculated. Nevertheless, no significant results could be found with those parameters as no differences were obtained from one product to another. As a consequence, only the pore size will be discussed in the present work.

3.2.2. Link between microstructure and sensitivity to a stress concentration

Once the pore sizes were extracted for all the slices of the XµCT results, a frequency distribution was drawn using for one sample all the pores of all the slices. Results shown below will focus on the big pores of the distribution. 10 different samples were analyzed

268   using this procedure. Two pressure points were chosen for each product. The first was

269   100 MPa for all the samples and the second was the pressure point that gave a global

270   porosity around 12.5% for the tablet, i.e. 200 MPa for all the products except for DCP for

271   which the pressure was 400MPa (cf. table 3).

272   First, the evolution of the pore size distribution as a function of the applied pressure was

273   monitored for each product. Results can be seen in figure 5. In each case, the pore size

274   distribution is shifted to lower sizes when the pressure increases and for each case, the

275   size of the largest defects decreases with increasing pressure. This result was expected

276   and can be used as a validation of the data treatment methodology used in this work.

277   Moreover, in the previous section of the article, we showed that increasing the pressure

278   increased the sensitivity to stress concentration for each product. This could be

279   explained by the fact that the pore size in the structure are smaller when the pressure

280   increases. Of course the global porosity is also different and the defects concentration

281   could also play a role in the sensitivity to stress concentration.

282   To separate the effect of global porosity and pore size, tablets with approximately the

283   same porosity were compared. The case of the tablets presented in table 3 was

284   considered. Pore size distribution for all the 5 tablets can be found in figure 6. It is

285   interesting to note that, as expected, even if these tablets have a similar global porosity,

286   the pore size distribution differs from one product to another. This confirms that global

287   porosity is not a sufficient descriptor of the tablet microstructure. But the most interesting

288   point is that there is a correlation between the pore size distribution and the sensitivity to

289   defects. If we compare the values of a_0 given in table 3 to the position of the pore size

290   distribution, we can see that the lower a_0, the smaller the size of the biggest pores. To

291   better visualize this fact, the mean diameter of the 10 largest defects in the structure

292   (noted $<D>_{10}$) was calculated for each tablet and is reported in table 3 along with a_0

293   values (the value of 10 was chosen arbitrarily for the sake of the demonstration).

294   Evolution of a_0 as a function of $<D>_{10}$ was then drawn on figure 7. Again, we can see

295   that the lower a_0, the lower the mean diameter of the largest pores.

296   These results show the strong correlation between the pore size and the sensitivity to a

297   stress concentration for the products considered in this studies. This sensitivity is directly

298   related to the microstructure itself, which is dependent on the deformation behavior of

299   the products under compression. This correlation does of course not mean that the

300   microstructure is the only parameter influencing the sensitivity to defects. Some material

301   related properties (i.e. surface energy) might also play a significant role and were not

302   included in the present study.

303   Moreover, it is worth noting here that the products studied in the present work present a

304   brittle fracture behavior during diametral compression. For other more ductile products

305   (e.g. microcrystalline cellulose), some other effects may take place (large plastic

306   deformation ahead the crack tip, etc.) that might render the correlation more

307   complicated. Present results might thus not be directly applicable to this kind of tablets.

308   Nevertheless, these results represent a first effort of explaining, from a more

309   fundamental point of view, the sensitivity of a tablet to the presence of defects.

310   **Conclusion**

311   In this work, 5 different pharmaceutical excipients were studied in terms of sensitivity to

312   a stress concentration. The average criterion method, developed in a precedent work,

was successfully applied to tablets of the different excipients made under several pressure points. Because it takes into account the size of the hole placed in the tablet, this criterion can be considered as a generalization of Hiestand's approach to characterize the sensitivity of a tablet to stress concentration.

Moreover, using XμCT, the microstructure of the tablets was studied. A special attention was paid to the size of the largest pores in the structure. Analysis of the pore size distribution for the different products showed a direct correlation between the size of the largest pores and the sensitivity to a stress concentration: the largest the defects, the lower the sensitivity. These results show the importance of the microstructure to explain the sensitivity to stress concentration and, as a consequence to understand the capping tendency of formulations. This study constitutes a first step in the fundamental understanding of the sensitivity to stress concentration of pharmaceutical tablets.

Legend to figures

Figure 1: photographs of the powder obtained under scanning electron microscope. Pictures were taken using a Hitachi TM 3000 (Hitachi, Tokyo, Japan). (a) DCP, (b) MLac, (c) ALac, (d) SDLac, (e) SDMan.

Figure 2: Localization of the sampling zone for X-ray tomography analysis: (a) top view; (b) side view.

Figure 3: Application of the average stress criterion to the different products : (a) DCP, (b) MLac, (c) ALac, (d) SDLac et (e) SDMan. $F_{applied}$ is the force needed to break the tablet with a hole and $F_{0\,applied}$ is the force needed to break the tablet without a hole.

Figure 4: Example of XμCT image before (left) and after (right) thresholding. Blue pixels on the right picture represent the pore structure that will be analyzed afterward

Figure 5: evolution of the pore size distribution with increasing pressure

Figure 6: pore size distribution for tablets with an global porosity around 12.5%.

Figure 7: evolution of a_0 as a function of the mean diameter of the 10 biggest defects in the structure.

Bibliography

[1] G. Alderborn, Tablets and compaction, in: Aultons Pharm. Des. Manuf. Med., Churchill Livingstone, London, 2001.

[2] U.S. Pharmacopeia, <1062> Tablet Compression Characterization, (2018).

[3] S.C. Gad, Pharmaceutical manufacturing handbook: production and processes, John Wiley & Sons, 2008.

[4] E.N. Hiestand, J.E. Wells, C.B. Peot, J.F. Ochs, Physical processes of tableting, J. Pharm. Sci. 66 (1977) 510–519.

[5] V. Mazel, H. Diarra, V. Busignies, P. Tchoreloff, Evolution of the Die-Wall Pressure during the Compression of Biconvex Tablets: Experimental Results and Comparison with FEM Simulation, J. Pharm. Sci. 104 (2015) 4339–4344.

[6] C.-Y. Wu, B. Hancock, A. Mills, A. Bentham, S. Best, J. Elliott, Numerical and experimental investigation of capping mechanisms during pharmaceutical tablet compaction, Powder Technol. 181 (2008) 121–129.

[7] J.M. Whitney, R.J. Nuismer, Stress Fracture Criteria for Laminated Composites Containing Stress Concentrations, J. Compos. Mater. 8 (1974) 253–265.

363 [8]   C. Imbert, P. Tchoreloff, B. Leclerc, G. Couarraze, Indices of tableting performance and application
364   of percolation theory to powder compaction, Eur. J. Pharm. Biopharm. 44 (1997) 273–282.
365 [9]   O.A. Itiola, N. Pilpel, Tableting characteristics of metronidazole formulations, Int. J. Pharm. 31
366   (1986) 99–105.
367 [10] S. Majuru, D.E. Wurster, The Effect of Composition on the Tableting Indices of Binary Powder
368   Mixtures, Pharm. Dev. Technol. 2 (1997) 313–321.
369 [11] R.S. Okor, F.E. Eichie, C.N. Ngwa, Correlation Between Tablet Mechanical Strength and Brittle
370   Fracture Tendency, Pharm. Pharmacol. Commun. 4 (1998) 511–513.
371 [12] R.J. Roberts, R.C. Rowe, Brittle fracture propensity measurements on 'tablet-sized' cylindrical
372   compacts, J. Pharm. Pharmacol. 38 (1986) 526–528.
373 [13] M.D. Schulze, J.W. McGinity, Indices of Tableting Performance for Acrylic Resin Polymers with
374   Plastic and Brittle Drugs, Drug Dev. Ind. Pharm. 19 (1993) 1393–1411.
375 [14] H.E.N. Hiestand, D.P. Smith, Indices of tableting performance, Powder Technol. 38 (1984) 145–159.
376   https://doi.org/10.1016/0032-5910(84)80043-1.
377 [15] X. Gong, C.C. Sun, A new tablet brittleness index, Eur. J. Pharm. Biopharm. 93 (2015) 260–266.
378   https://doi.org/10.1016/j.ejpb.2015.04.007.
379 [16] X. Gong, S.-Y. Chang, F. Osei-Yeboah, S. Paul, S.R. Perumalla, L. Shi, W.-J. Sun, Q. Zhou, C.C. Sun,
380   Dependence of tablet brittleness on tensile strength and porosity, Int. J. Pharm. 493 (2015) 208–
381   213. https://doi.org/10.1016/j.ijpharm.2015.07.050.
382 [17] S. Paul, C.C. Sun, Lubrication with magnesium stearate increases tablet brittleness, Powder
383   Technol. 309 (2017) 126–132. https://doi.org/10.1016/j.powtec.2016.12.012.
384 [18] J.M. Sonnergaard, A New Brittleness Index for Compacted Tablets, J. Pharm. Sci. 102 (2013) 4347–
385   4352. https://doi.org/10.1002/jps.23741.
386 [19] P. York, F. Bassam, R.C. Rowe, R.J. Roberts, Fracture-Mechanics of Microcrystalline Cellulose
387   Powders, Int. J. Pharm. 66 (1990) 143–148.
388 [20] B. Croquelois, J. Girardot, J.B. Kopp, C. Cazautets, P. Tchoreloff, V. Mazel, Breaking pharmaceutical
389   tablets with a hole: Reevaluation of the stress concentration factor and influence of the hole size,
390   Powder Technol. 317 (2017) 126–132.
391 [21] V. Busignies, B. Leclerc, P. Porion, P. Evesque, G. Couarraze, P. Tchoreloff, Quantitative
392   measurements of localized density variations in cylindrical tablets using X-ray microtomography,
393   Eur. J. Pharm. Biopharm. 64 (2006) 38–50.
394 [22] D. Markl, A. Strobel, R. Schlossnikl, J. Bøtker, P. Bawuah, C. Ridgway, J. Rantanen, T. Rades, P. Gane,
395   K.-E. Peiponen, J.A. Zeitler, Characterisation of pore structures of pharmaceutical tablets: A review,
396   Int. J. Pharm. 538 (2018) 188–214.
397 [23] D. Markl, P. Wang, C. Ridgway, A.-P. Karttunen, M. Chakraborty, P. Bawuah, P. Pääkkönen, P. Gane,
398   J. Ketolainen, K.-E. Peiponen, J.A. Zeitler, Characterization of the Pore Structure of Functionalized
399   Calcium Carbonate Tablets by Terahertz Time-Domain Spectroscopy and X-Ray Computed
400   Microtomography, J. Pharm. Sci. 106 (2017) 1586–1595.
401 [24] A.M. Miguélez-Morán, C.-Y. Wu, H. Dong, J.P.K. Seville, Characterisation of density distributions in
402   roller-compacted ribbons using micro-indentation and X-ray micro-computed tomography, Eur. J.
403   Pharm. Biopharm. 72 (2009) 173–182.
404 [25] K. Kendall, A.J. Howard, J.D. Birchall, P.L. Pratt, B.A. Proctor, S.A. Jefferis, P.B. Hirsch, J.D. Birchall,
405   D.D. Double, A. Kelly, G.K. Moir, C.D. Pomeroy, The relation between porosity, microstructure and
406   strength, and the approach to advanced cement-based materials, Philos. Trans. R. Soc. Lond. Ser.
407   Math. Phys. Sci. 310 (1983) 139–153.
408 [26] V.D. Krstic, Effect of microstructure on fracture of brittle materials: Unified approach, Theor. Appl.
409   Fract. Mech. 45 (2006) 212–226.

410   [27]   V. Mazel, S. Guerard, B. Croquelois, J.-B. Kopp, J. Girardot, H. Diarra, V. Busignies, P. Tchoreloff,
411   Reevaluation of the diametral compression test for tablets using the flattened disc geometry, Int. J.
412   Pharm. 513 (2016) 669–677.

413   [28]   A.-N. Spiess, N. Neumeyer, An evaluation of R2 as an inadequate measure for nonlinear models in
414   pharmacological and biochemical research: a Monte Carlo approach, BMC Pharmacol. 10 (2010) 6.

415   [29]   T.O. Kva°Lseth, Note on the R2 measure of goodness of fit for nonlinear models, Bull. Psychon. Soc.
416   21 (1983) 79–80. https://doi.org/10.3758/BF03329960.

417   [30]   H.S. Bennett, J.J. Filliben, A Systematic Approach for Multidimensional, Closed-Form Analytic
418   Modeling: Effective Intrinsic Carrier Concentrations in Ga1−xAlxAs Heterostructures, J. Res. Natl.
419   Inst. Stand. Technol. 107 (2002) 69–81. https://doi.org/10.6028/jres.107.008.
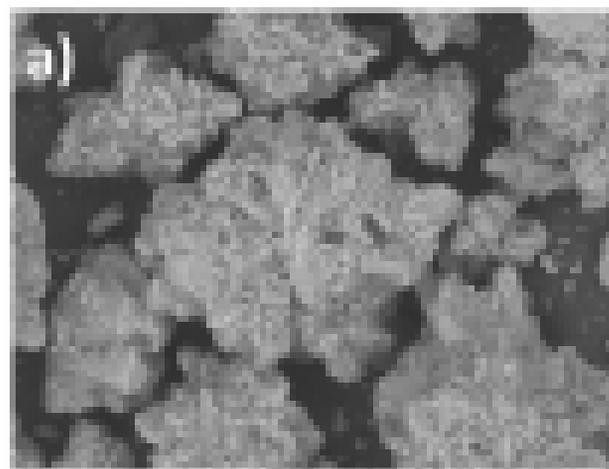
420
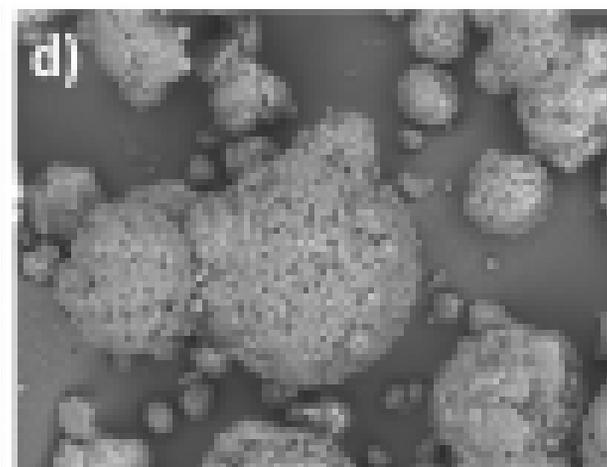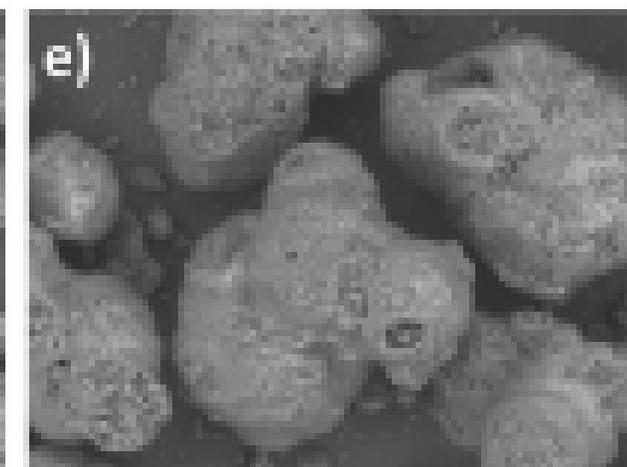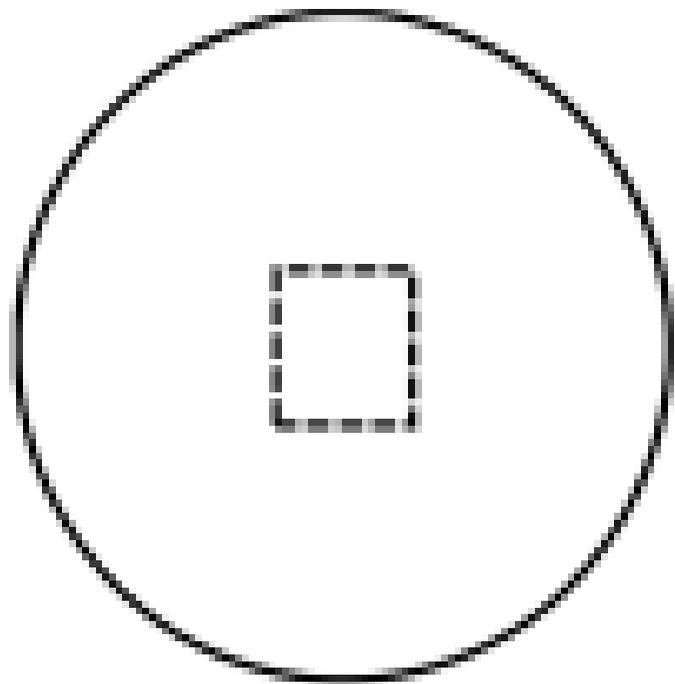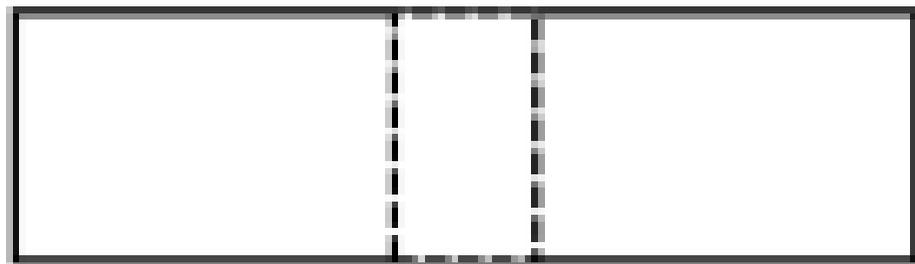
(a)   (b)
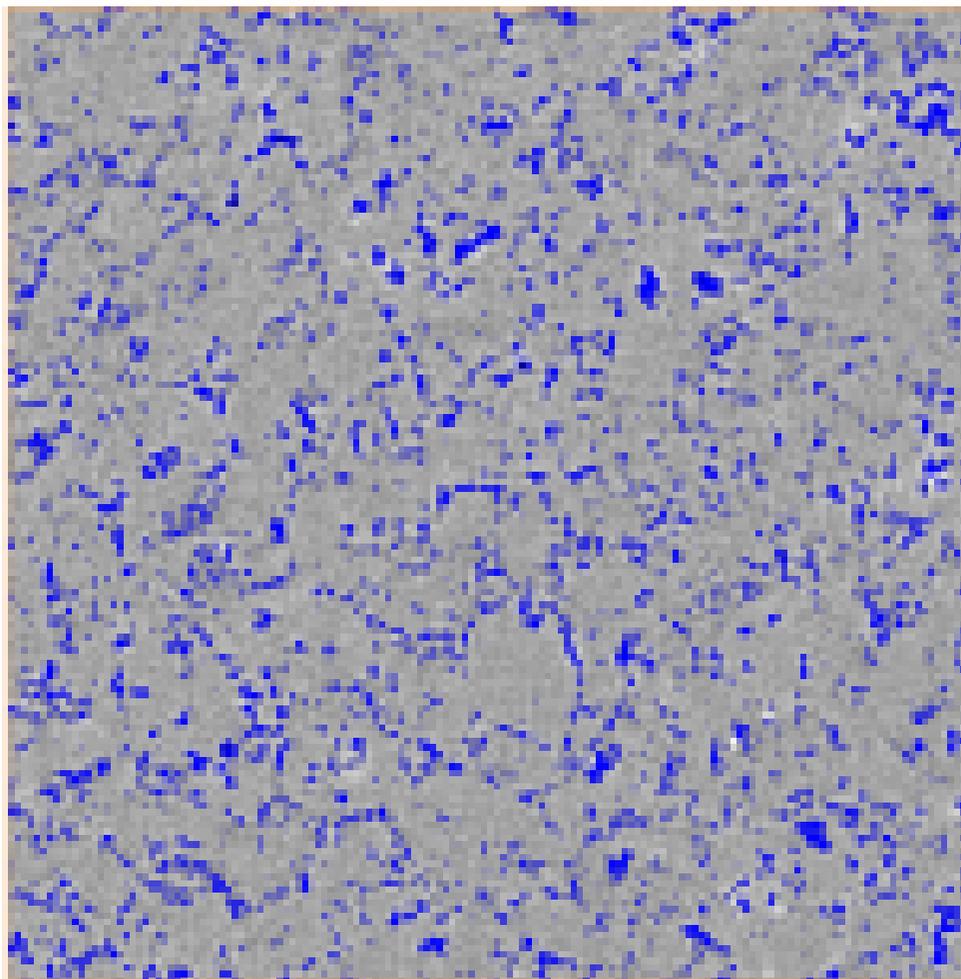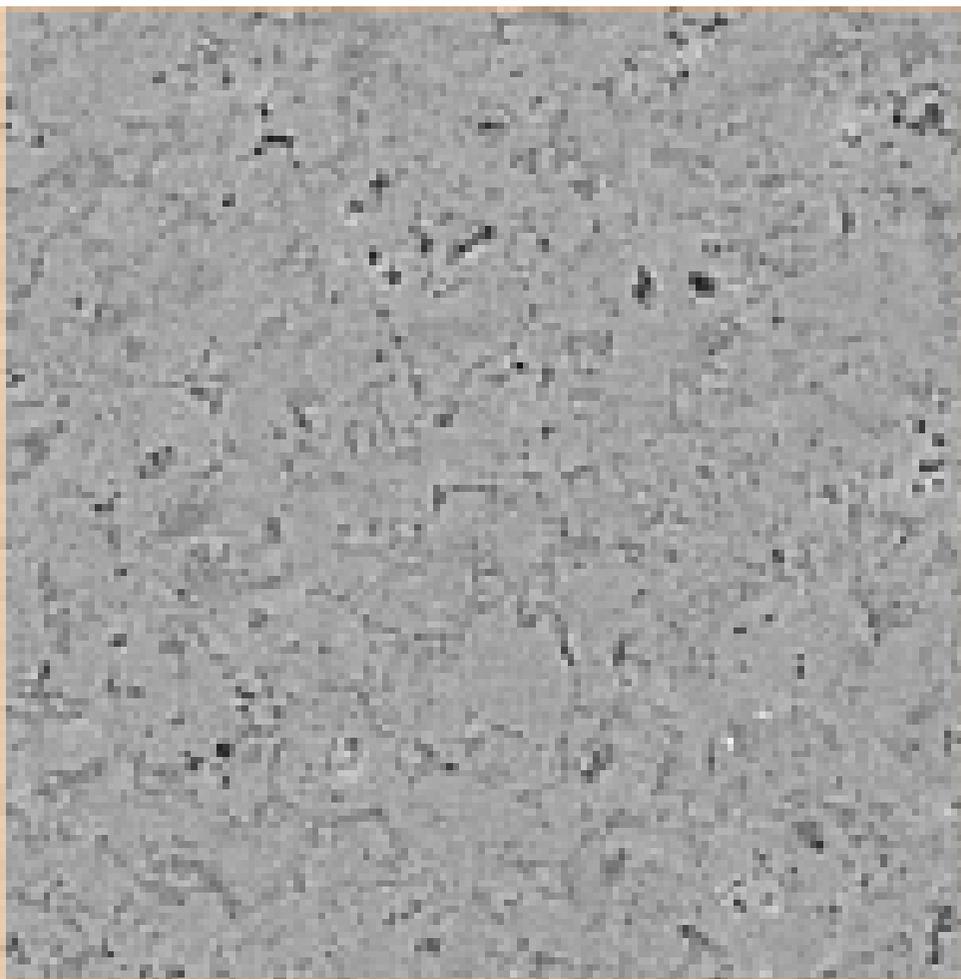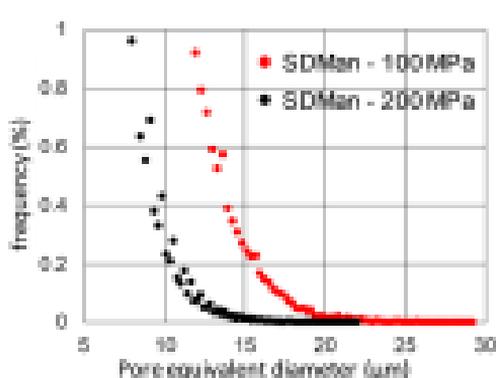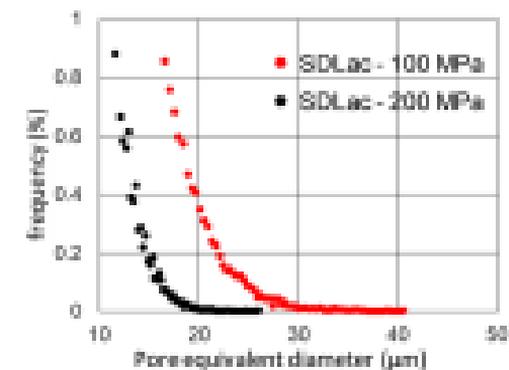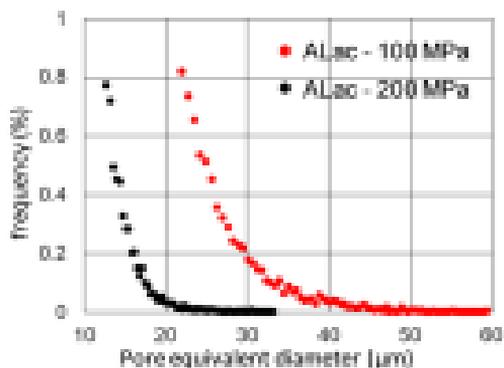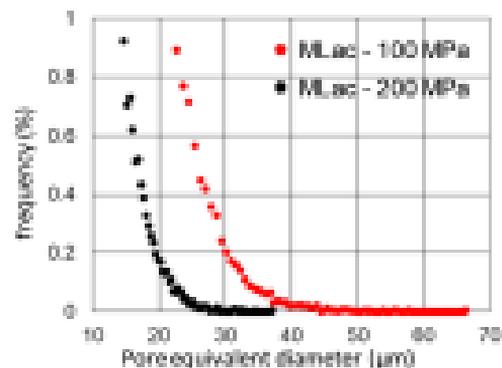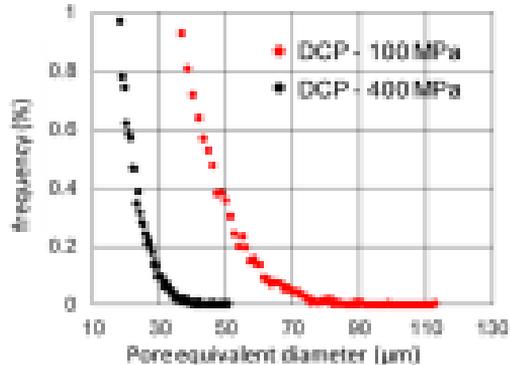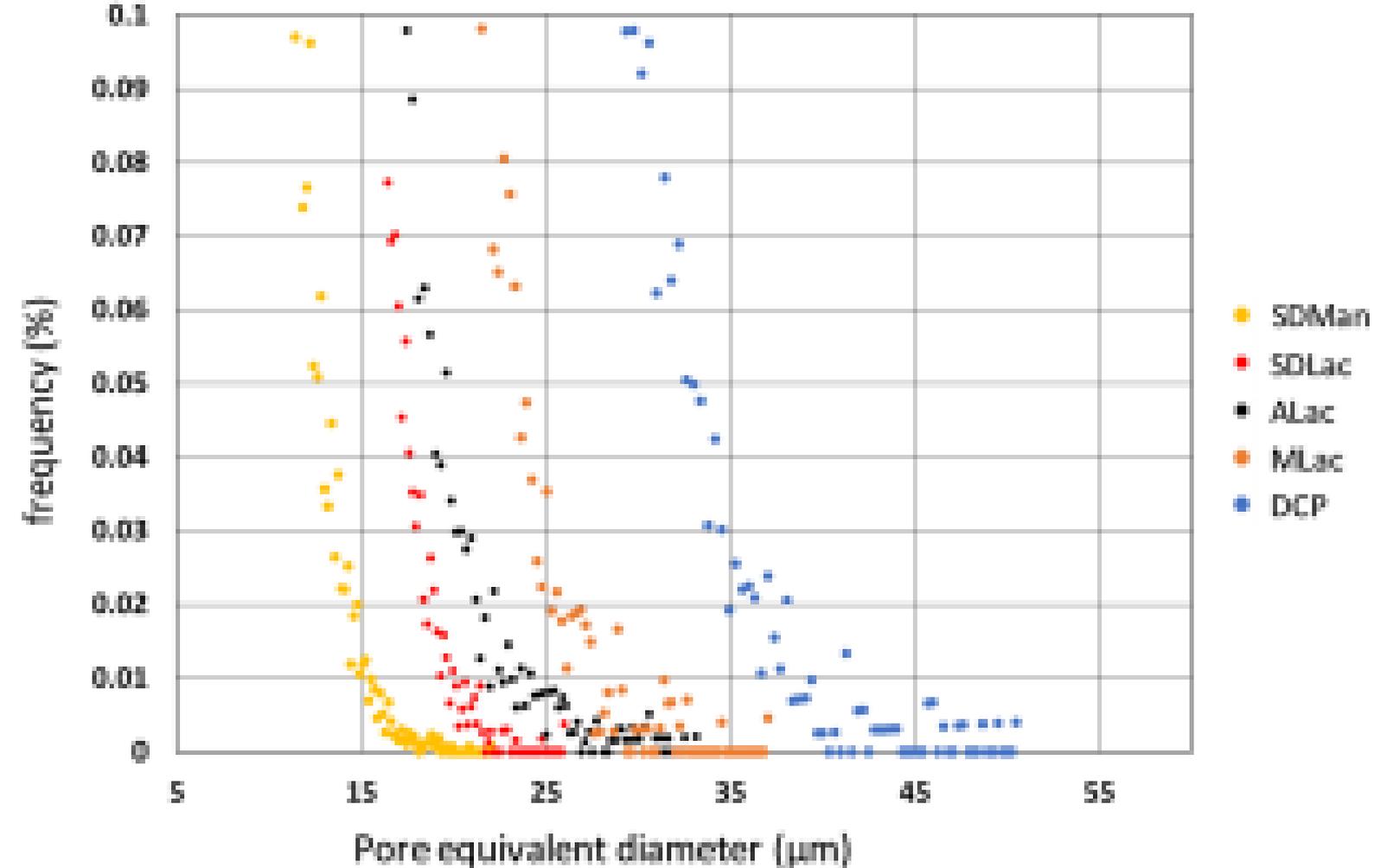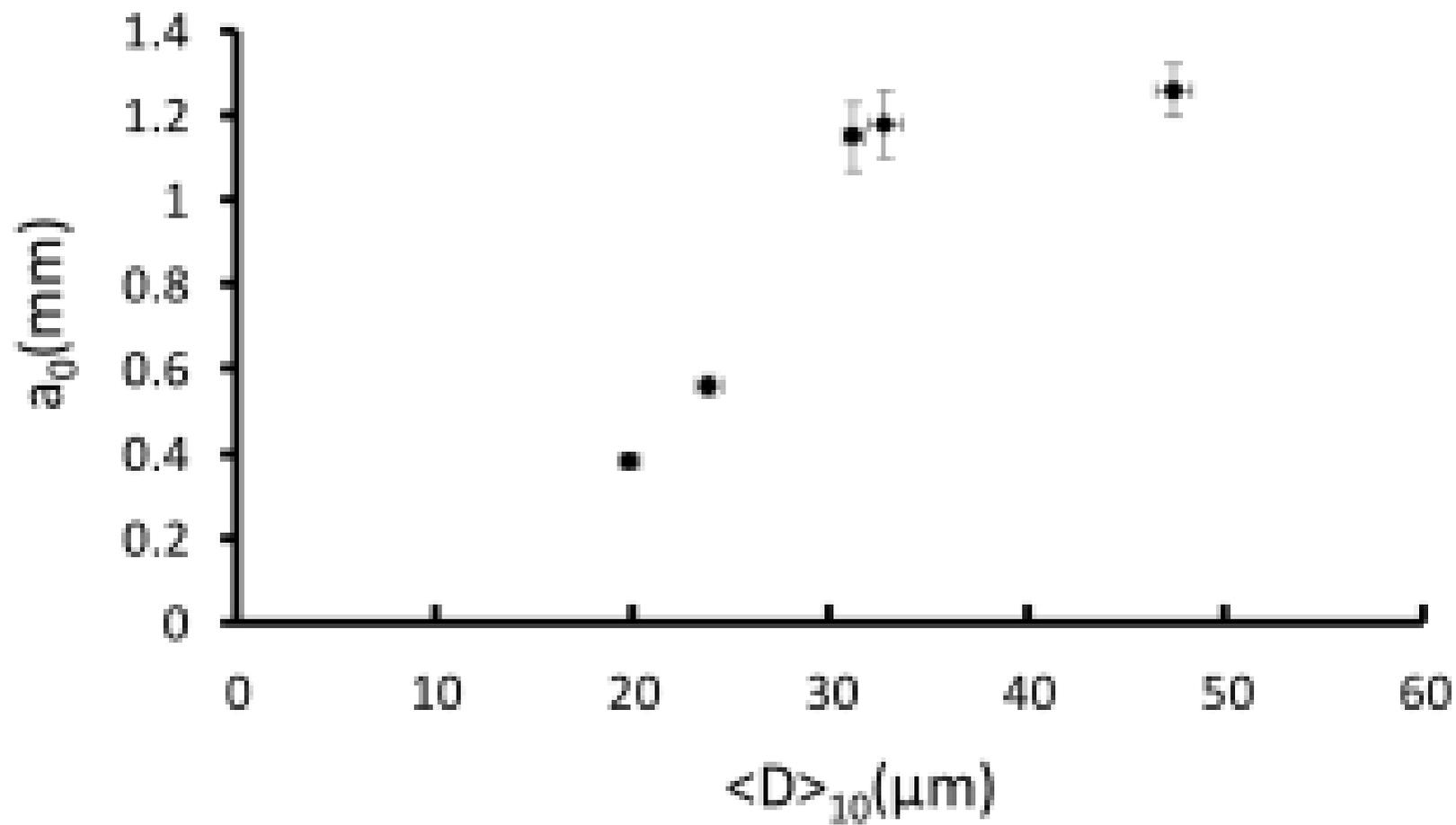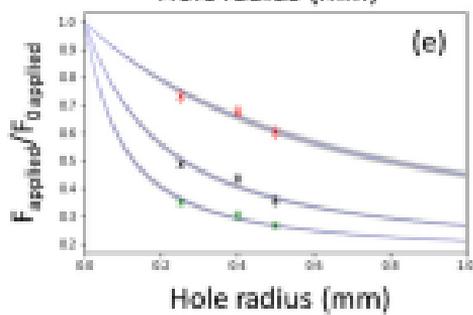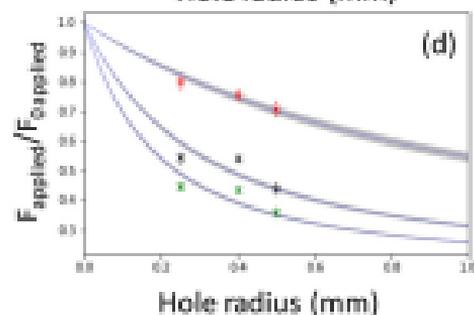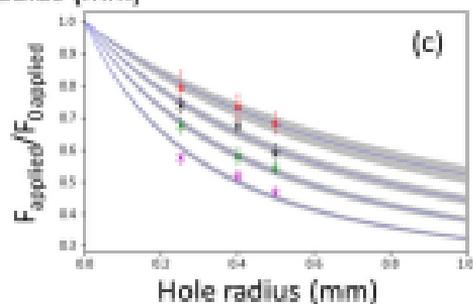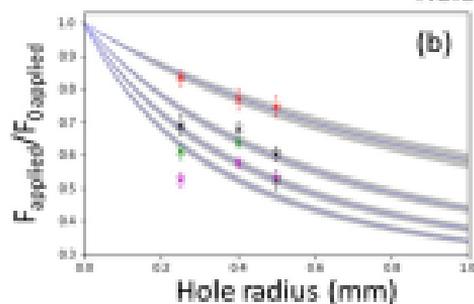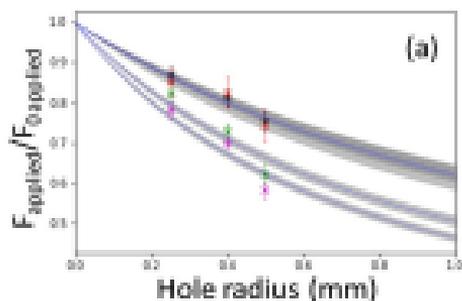
(X) 100 MPa (X) 200 MPa (X) 300 MPa (X) 400 MPa

Table 1: Parameters of the particle size distribution of the powders used in the present study. The analysis were performed by laser diffraction using a Mastersizer 2000 (Malvern, Malvern, UK). All parameters were measured on the volume distribution.

Product	Mean diameter (µm)	D_{10} (µm)	D_{50} (µm)	D_{90} (µm)
DCP	209	120	196	316
Alac	181	37	165	342
Mlac	153	52	136	281
SDMan	156	98	155	235
SDLac	140	52	129	241

Table 2: value of a_0 parameter and porosity for each product and each pressure point. Se is the residual standard deviation.

Product	Pressure	a_0(mm)			Se	Porosity (%)
DCP	100	2.44	±	0.35	$2.4 \cdot 10^{-2}$	23.2
	200	2.55	±	0.22	$1.3 \cdot 10^{-2}$	18.1
	300	1.51	±	0.1	$3.8 \cdot 10^{-2}$	15.1
	400	1.26	±	0.06	$3.7 \cdot 10^{-2}$	13.4
Alac	100	1.63	±	0.2	$1.4 \cdot 10^{-2}$	17.7
	200	1.15	±	0.08	$2.0 \cdot 10^{-2}$	11.3
	300	0.85	±	0.047	$1.1 \cdot 10^{-2}$	8.7
	400	0.59	±	0.025	$3.0 \cdot 10^{-2}$	7.1
Mlac	100	2.14	±	0.22	$1.2 \cdot 10^{-2}$	18.1
	200	1.18	±	0.08	$4.4 \cdot 10^{-2}$	12
	300	0.82	±	0.05	$6.7 \cdot 10^{-2}$	9.1
	400	0.7	±	0.038	$7.1 \cdot 10^{-2}$	7.1
SDMan	100	1.18	±	0.07	$2.0 \cdot 10^{-2}$	21.3
	200	0.38	±	0.018	$2.6 \cdot 10^{-2}$	13.8
	300	0.19	±	0.011	$1.2 \cdot 10^{-2}$	9.3
SDLac	100	1.82	±	0.13	$1.7 \cdot 10^{-2}$	20.3
	200	0.56	±	0.024	$5.2 \cdot 10^{-2}$	12.4
	300	0.36	±	0.013	$4.4 \cdot 10^{-2}$	8.9

Table 3: Value of a_0 and $<D>_{10}$ for product having an overall porosity around 12.5%. $<D>_{10}$ is the mean diameter of the 10 largest pores in the structure as found by xμCT.

Product	Pressure	a_0(mm)			Porosity (%)	$<D>_{10}$(μm)		
DCP	400	1.26	±	0.06	13.4	47.4	±	0.87
Alac	200	1.15	±	0.08	11.3	31.2	±	0.5
Mlac	200	1.18	±	0.08	12	32.8	±	0.9
SDMan	200	0.38	±	0.018	13.8	19.9	±	0.5
SDLac	200	0.56	±	0.024	12.4	23.9	±	0.65